

# Factors Associated with Dough Stickiness as Sensed by Attenuated Total Reflectance Infrared Spectroscopy

Ewoud J. J. van Velzen,<sup>1,2</sup> John P. M. van Duynhoven,<sup>1</sup> Paul Pudney,<sup>3</sup>  
Peter L. Weegels,<sup>1</sup> and John H. van der Maas<sup>4</sup>

## ABSTRACT

Cereal Chem. 80(4):378–382

Attenuated total reflectance (ATR) and Fourier transform infrared (FTIR) spectroscopy have been applied in the characterization of sticky dough surfaces. The characterization provides insight in the chemical distribution of gluten protein, starch, water, and fat during dough kneading. ATR is especially useful for selective sampling of dough surfaces because the depth of penetration of radiation is quite shallow. For dough, it is calculated to be in the order of 0.5–4  $\mu\text{m}$  in the mid-infrared, ideal for measurements of stickiness effects, where only the dough surface is of interest. To investigate the cohesive and adhesive properties of the individual dough constituents, dough was peeled from the ATR plate to study the material that adhered to it. The infrared spectra obtained indicate that fat and gluten protein appear to be located at the outer sticky dough surfaces, rather than water and starch. In comparison with gluten, the fatty component showed relatively strong

adhesive forces to the ATR plate; a high residual fraction was measured after peeling the dough. Gluten proteins display different cohesion and adhesion properties that are strongly dependent on their hydration state. This indicates that the degree of hydration of gluten proteins contributes to the sticky properties of (overkneaded) dough. When analyzing gluten protein in  $\text{D}_2\text{O}$  instead of a dough matrix, more or less similar results were obtained. Significant differences in amide I and amide II intensities were measured for kneaded and stretched gluten protein in comparison to untreated, wet gluten. Besides changes in the vibrational properties of the amide groups, conformational changes in the tertiary protein structure also were observed. It appears that kneading and stretching of dough results in a major decrease in  $\alpha$ -helices content, accompanied by an increase of extended  $\beta$ -sheet conformations.

According to Chen and Hosoney (1995) and Hosoney and Smewing (1999), “the rheologist Scott Blair (1936) neatly summed up the problem of dough stickiness over 60 years ago when he stated that stickiness appears to be the property of dough to which the baker’s hand is most sensitive.” Today, when dough is handled more by machine and less by the baker’s hand, the importance of sticky dough is even greater. Dough that is sticky can cause immense problems in the mechanical breadmaking process. Dusting flour, up to 5% of the total flour, is sometimes used to overcome stickiness. However, the consequence of adding flour generates significantly higher production costs. Although the impact of the efficiency loss is severe, the fundamental knowledge and controlling dough stickiness is still limited. To understand the phenomenon of stickiness better as a result of prolonged kneading, a spectroscopic study has been performed. However, many other processing and formulation variables can contribute to stickiness as well (e.g., kneading temperature, protein composition, pentosan content). These variables were not evaluated in the present study.

Even though sticky doughs have been a problem ever since humans first started making dough, it received limited scientific study until recently. Previous studies have linked a number of factors to dough stickiness. These include the amount of water-soluble pentosans, differences in protein composition,  $\alpha$ -amylase activity, and proteolytic activity (Chen and Hosoney 1995; Hosoney and Smewing 1999). However, these studies of factors affecting dough stickiness were all hampered by lack of an objective test to measure stickiness. Chen and Hosoney (1995) and Hosoney and Smewing (1999) reported studies focused on factors affecting the adhesion properties of dough. Sequential separation, fractionation, and reconstitution techniques were used to show that the entity that caused the dough to be sticky (adhesive) was water-soluble and of relatively small size. The compound was identified as ferulic

acid, esterified to a hexose chain. It was also shown that saponification of the ester bond destroyed the ability of the entity to cause a sticky dough.

Although the exact nature of stickiness is still unknown, one of the most likely hypotheses starts from the idea that water undergoes redistribution during kneading, thus altering the hydration state of the gluten phase. The water-redistribution phenomenon and the hydration of gluten have also been studied by spectroscopic methods. Fourier transform infrared (FTIR) spectroscopy has shown that the gluten amide absorptions undergo intensity changes during kneading that have been attributed to hydration.

Stickiness is a surface-related characteristic to which human skin is sensitive. This property can be defined as the force of adhesion when two surfaces are in contact with each other. In dough matrices, the adhesion force is a combination of an adhesive force and a cohesive force. It is when the adhesive force is high and the cohesive force is low that the dough is perceived as being sticky (Hosoney and Smewing 1999). Dobraszczyk (1997) states that the cohesive energy term is usually the major contribution to the measured adhesive fracture energy and is generally highly dependent on the viscoelastic properties of the adhesive. Therefore, stickiness is not a constant material property but is principally dependent on the viscoelastic rheological properties of the adhesive and, as such, will be dependent on the imposed rate, temperature, and size of the deformation.

To study rheological-chemical relationships at sticky dough surfaces, it is essential to use analytical techniques with the ability to collect chemical information specifically from the outer micrometer layers. Furthermore, a crucial limiting factor is the restricted exposure time with air to prevent time-related variables such as changes in temperature and humidity, evaporation of water, and proofing. In this context, FTIR spectroscopy is probably one of the most convenient and straightforward analytical tools to get the chemical information. In FTIR, the presence of functional groups (e.g., amide groups in protein) is determined either qualitatively or quantitatively. This is accomplished by detecting the absorption of infrared light in the wavelength range between 2.5 and 25  $\mu\text{m}$  ( $4,000\text{--}400\text{ cm}^{-1}$ ). The frequency of the light that is absorbed is characteristic for the presence of a specific functional group or chemical bond type. The frequency of the light that a specific bond will absorb depends on the chemical environment in which the

<sup>1</sup> Unilever Research, P.O. Box 114, 3130 AC Vlaardingen, The Netherlands.

<sup>2</sup> Corresponding author. E-mail: Ewoud-van.Velzen@unilever.com.

<sup>3</sup> Unilever Research, Colworth House Sharnbrook, Bedford MK44 1LQ, United Kingdom.

<sup>4</sup> Infrared and Raman Group, Utrecht University, Sorbonnelaan 16, 3584 CA Utrecht, The Netherlands.

functional group or chemical bond is contained. For example the amide peptide bonds in gluten proteins with an  $\alpha$ -helix conformation adsorb light in the frequency of 1,650–1,655  $\text{cm}^{-1}$ , whereas amide peptide bonds in a  $\beta$ -sheet conformation adsorb light at 1,620–1,640  $\text{cm}^{-1}$  (Byler et al 1986; Mantsch and Casal 1986; Wharton 1986). An attenuated total reflection (ATR) accessory was used for measuring dough surfaces of different states of stickiness within the first micrometer layers as well as the conformational behavior of gluten protein as a result of kneading, stretching, and hydration.

### ATR Infrared Spectroscopy

In ATR, the samples are put on to an infrared transparent crystal of high refractive index (internal reflectance element [IRE]) that permits almost total internal reflectance. ATR has been applied for dough and gluten protein measurements because it offers some important benefits. The main characteristic of ATR is its surface sensitivity, which results from the phenomenon of the evanescent infrared wave, established between the reflecting ATR crystal and the sample, penetrating only a few micrometers into the sample. The small penetration depth of the evanescent wave requires a close contact between the crystal and the sample to obtain the sample's infrared spectrum. The depth of penetration ( $D_p$ ) of the incident infrared radiation depends on the angle of incidence ( $\theta$ ), the frequency of incident light at any specific wavelength  $\lambda$ , and the refractive index difference between ATR element ( $\eta_1$ ) and the dough sample ( $\eta_2$ ) (Harrick 1979; Wilson 1990; van de Voort and Ismail 1991; Dupuy et al 1994; Martin 1999). Depth profiling is feasible using different ATR crystals with increasing angles of incidence ( $\theta$ ). In the following equation,  $D_p$  is defined as the distance required for the amplitude of the incident wavelength ( $\lambda$ ) to fall to an  $e^{-1}$  value:

$$D_p = \frac{\lambda}{2\pi \cdot \eta_1 \cdot \sqrt{\sin^2 \theta - \left(\frac{\eta_2}{\eta_1}\right)^2}} \quad (1)$$

Another advantage of the ATR approach is that the sample surface is protected from the atmosphere. Direct contact between the dough and the ATR plate implies that chemical and physical changes will be restricted during the infrared acquisition time. Furthermore, the 'boat' design of the ATR plate permits the addition of extra solvent ( $\text{H}_2\text{O}$  and  $\text{D}_2\text{O}$ ) to prevent dehydration.

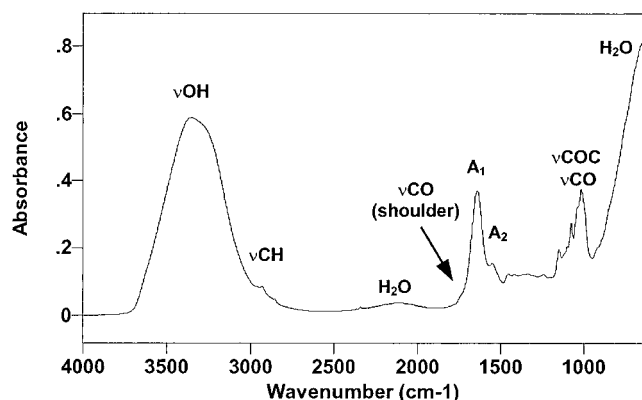


**Fig. 1.** Attenuated total reflectance (ATR) and Fourier transform infrared (FTIR) spectrum of optimally developed Baguepi dough (kneaded for 13 min) collected on a ZnSe ATR crystal with a  $60^\circ$  angle of incidence. vCH, aliphatic CH stretching of  $\text{CH}_2$  and  $\text{CH}_3$  (fat); vCO, carbonyl stretching of the fat triglyceride ester linkage;  $A_1$ , carbonyl stretching of the gluten protein (amide I) in combination with the OH deformation of water;  $A_2$ , NH bending and CH stretching of gluten protein (amide II); vCOC/vCO, C-O-C stretching and CO (-COH) stretching of starch (Workman 2001).

## MATERIALS AND METHODS

### Sample Preparation and Handling

Dough samples were prepared for Baguepi flour (Moulins de Soufflet Pantin, France) with 1.4% (w/w) salt, 4.4% (w/w) yeast, 0.2% (w/w) bread improver (Congel, Astra Calve, France), and 36% (w/w) water and kneaded in a spiral mixer (Diosna Dierks & Söhne GmbH, Germany) for 2 and 25 min to obtain nonsticky and sticky dough. During kneading, the temperature was kept constant at  $20 \pm 0.5^\circ\text{C}$  with a temperature controlled  $\text{CO}_2$  cooling purge. The freshly prepared dough samples (0.5 cm thick) were carefully positioned on a horizontal zinc selenide (ZnSe) ATR plate with minimal stress and shear forces. Immediately after acquisition, each sample was removed from the plate in one flowing move to have a more or less reproducible residue left on the horizontal ATR plate. After removing the bulk of the dough, a second infrared measurement was performed on the remaining material. Each of the FTIR experiments were performed within 10 min of sample preparation to prevent molecular and structural changes as much as possible. All experiments were repeated once to estimate the reproducibility of the obtained results.

Gluten protein samples were prepared in  $\text{D}_2\text{O}$  with 34% dry vital gluten protein (Avebe, The Netherlands) and kneaded for 1 and 13 min using a Brabender Farinograph to investigate conformational changes in the secondary gluten protein structure as a result of kneading (Table I). During kneading, the temperature was kept at  $20$ – $25^\circ\text{C}$ . Like the dough samples, the prepared gluten protein were carefully positioned (without stretching) on a ZnSe ATR plate and covered with  $\text{D}_2\text{O}$  to prevent dehydration. In a second experiment, infrared measurements of the gluten protein samples were collected while applying static stretch. To achieve this, a piece of the gluten protein was stretched out and fixed to a ZnSe ATR plate using an ATR clamp (SpectraTech).

### Infrared Measurements

ATR FTIR experiments were performed on a spectrometer (FTS-6000, Bio-Rad, Cambridge, MA) equipped with a deuterated tri-glycine sulfate (DTGS) detector. For both sample and background, 64 asymmetric interferograms with a spatial resolution of  $4 \text{ cm}^{-1}$  were co-added and Fourier-transformed. Based on the symmetric peak shapes in the resulting infrared spectra, it was not necessary to phase-correct the asymmetric data set. WinIR-Pro (v. 2.9, Bio-Rad) and GRAMS/32 (v. 5.0, Galactic) software were used for acquisition and spectral processing, respectively. The samples were measured on an ATR accessory (SpectraTech) with three zinc selenide (ZnSe) crystals each possessing a different angle of incidence ( $\theta$ ):  $40^\circ$ ,  $45^\circ$ , and  $60^\circ$ . The single-beam spectrum of each sample was ratiomed against the reference single-beam spectrum of the clean ATR crystal.

**TABLE I**  
Experimental Conditions of Gluten Protein in  $\text{D}_2\text{O}$

Experiment	Gluten Protein in $\text{D}_2\text{O}$	Kneaded <sup>a</sup>	Stretched
1	Yes	No	No
2	Yes	Yes	No
3	Yes	No	Yes
4	Yes	Yes	Yes

<sup>a</sup> Kneading times: 1 min (underkneaded) and 13 min (overkneaded).

**TABLE II**  
Characteristic Frequencies ( $\text{cm}^{-1}$ ) and Assignments of Four Main Amide I Components<sup>a</sup>

Wavenumber ( $\text{cm}^{-1}$ )	Assignment
$1,675 \pm 5$	$\beta$ -Turn
$1,653 \pm 4$	$\alpha$ -Helix
$1,633 \pm 5$	Extended $\beta$ -sheet
$1,618 \pm 10$	Intermolecular $\beta$ -sheet (due to aggregation)

<sup>a</sup> Workman (2001).

## Curve Fitting

To investigate the spectral changes within the complex infrared spectra, the use of curve-fitting techniques (Byler et al 1986) is practically inevitable. In this mathematical approach, a number of Gaussian curves are fitted to a set of overlapping peaks. For the spectral region 1,800–1,500  $\text{cm}^{-1}$ , it is essential to resolve three overlapping bands at 1,745  $\text{cm}^{-1}$  (C=O stretch), 1,640  $\text{cm}^{-1}$  (C=O stretch of amide I and OH bend), and 1,550  $\text{cm}^{-1}$  (amide II, NH bend/CN stretch) into separate peaks. These infrared bands can be associated with fat, gluten protein and water, and gluten protein, respectively (Workman 2001). Iterative data processing was performed with GRAMS/32 software and the Array-Basic modules ‘Curve Fitting’ and ‘Peak Integration.’ In the iterative curve-fitting procedure, the bandwidths of the infrared absorptions at 1,745, 1,640, and 1,550  $\text{cm}^{-1}$  were initially set to realistic starting values (i.e., 22, 76, and 50  $\text{cm}^{-1}$ , respectively).

Curve fitting is also used to investigate conformational changes in the secondary protein structure of gluten under varying experimental conditions in  $\text{D}_2\text{O}$  (Table II). The use of  $\text{D}_2\text{O}$  is an important prerequisite because  $\text{H}_2\text{O}$  is characterized by a strong overlapping absorption with the carbonyl stretching band of gluten protein at  $\approx 1,640 \text{ cm}^{-1}$ . Because the carbonyl absorption (C=O stretch, amide I band) provides a sensitive probe for the secondary protein structure, the absence of overlapping bands is evident. To evaluate the major structure elements in the secondary protein conformation, curve-fitting techniques are required. According to the curve-fitting procedure described by Pezolet et al (1992), the amide I band can be resolved into four separate peaks. These separated peaks can be associated with distinct segments of the peptide backbone that represent different conformations: intermolecular  $\beta$ -sheets (1,612  $\text{cm}^{-1}$ ), extended  $\beta$ -sheets (1,631  $\text{cm}^{-1}$ ),  $\alpha$ -helices (1,650  $\text{cm}^{-1}$ ), and  $\beta$ -turns (1,668  $\text{cm}^{-1}$ ). During iterative curve-fitting, the bandwidths of the 1,612, 1,631, 1,650, and 1,668  $\text{cm}^{-1}$  peaks were initially set to realistic starting values (i.e., 33, 40, 27, and 29  $\text{cm}^{-1}$ , respectively). Dividing the sum of the calculated areas of all components associated with a given conformation by the total amide I band area gives a number that indicates what fraction of the protein has this particular conformation (Byler et al 1986; Tatham et al 1990; Pezolet et al 1992; Popineau et al 1994; Mangavel et al 1998; Belton 1999). It should be mentioned that this experiment is based on the assumption that the conformational behavior of gluten proteins in  $\text{D}_2\text{O}$  is more or less similar to

**TABLE III**  
Position, Peak Assignment, and Quantification  
of Selected Infrared Bands Representative of Spectral Markers  
for Individual Dough Constituents<sup>a</sup>

Peak Limits ( $\text{cm}^{-1}$ )	Assignment <sup>b</sup>	Calculation of Peak Area
2,150 $\pm$ 300	$\delta_{\text{def}}$ OH (water)	Integration
1,745 $\pm$ 30	$\nu$ CO (ester of fat)	Integration and curve fitting
1,640 $\pm$ 100	$\nu$ CO (amide I), $\delta_{\text{bend}}$ OH(water)	Integration and curve fitting
1,550 $\pm$ 65	$\delta_{\text{bend}}$ NH / $\nu$ CN (amide II)	Integration and curve fitting
1,070 $\pm$ 120	$\nu$ CO / $\nu$ COC (starch)	Integration

<sup>a</sup> Workman (2001).

<sup>b</sup>  $\delta$ : Group vibrational bending modes (or deformations);  $\nu$ : group vibrational stretching modes.

**TABLE IV**  
Penetration Depth ( $D_p$ ) of Infrared Radiation Through Dough Surface  
Depending on Angle of Incidence ( $\theta$ : 40, 45, and 60°) and Wavelength

Wavelength ( $\text{cm}^{-1}$ )	$\lambda$ ( $\mu\text{m}$ )	$D_p^a$ ( $\mu\text{m}$ )
2,150	4.65	2.1, 0.9, and 0.5
1,745	5.73	2.5, 1.1, and 0.6
1,640	6.10	2.7, 1.2, and 0.7
1,550	6.45	2.8, 1.3, and 0.7
1,070	9.35	4.1, 1.9, and 1.0

<sup>a</sup> Refractive index ( $\eta_1$ ) for ZnSe ATR element = 2.4. Index for dough samples ( $\eta_2$ )  $\approx$  1.5 on average (see Eq. 1).

that in  $\text{H}_2\text{O}$  because both solvents possess corresponding liquid properties, volume properties, densities, and dielectric constants at room temperature.

## RESULTS

### Chemical Characterization of Dough Surfaces

As illustrated in Fig. 1, the infrared spectrum of Baguepi dough developed to optimum mixing time (13 min) shows strong and distinctive absorption bands of the main constituents. Gluten protein, water, fat, and starch can easily be identified due to favorable infrared activities. Water has characteristic infrared features at  $\approx 3,350 \text{ cm}^{-1}$  (OH stretch), 1,640  $\text{cm}^{-1}$  (OH bend), 2,150  $\text{cm}^{-1}$  (OH def), and  $<800 \text{ cm}^{-1}$  (OH def). The infrared absorption bands of starch are at 1,020, 1,080, and 1,150  $\text{cm}^{-1}$ , and can be associated with the coupled C-O and C-C stretching vibrations (C-O/C-C stretch) of the polysaccharide molecules. Finally, fat displays some weak absorptions at 2,958  $\text{cm}^{-1}$  (asymmetric stretch of  $\text{CH}_3$ ), 2,928  $\text{cm}^{-1}$  (asymmetric stretch of  $\text{CH}_2$ ), and 2,854  $\text{cm}^{-1}$  (symmetric stretch of  $\text{CH}_2$ ) that can be assigned to the aliphatic fatty acid chains. Furthermore, the carbonyl stretching of the fatty ester groups can be distinguished at 1,743  $\text{cm}^{-1}$ . Typical protein absorption bands of amide I and amide II appear at 1,651  $\text{cm}^{-1}$  (C=O stretch) and 1,541  $\text{cm}^{-1}$  (NH bend/CN stretch), respectively. The amide I band, however, is strongly overlapped by the OH deformation band of water (OH bend). No water-subtracted spectrum is calculated because water is one of the crucial dough ingredients to look for in connection with dough stickiness. Instead of water subtraction, curve fitting is applied to resolve the overlapping bands in the spectral region 1,800–1,500  $\text{cm}^{-1}$  (Fig. 2).

To be able to compare water, gluten protein, fat, and starch distributions at different dough surfaces, relative peak areas were calculated from typical spectral markers, each representing another constituent (Table III).

Chemical effects as an effect of kneading were studied for dough surfaces at varying penetration depths ( $D_p$ ) using four different ZnSe ATR crystals. Depending on the wavelength ( $\lambda$ ) and the angle of incidence ( $\theta$ ) of the ATR plates, depth profiling experiments were performed (Table IV). A similar approach was performed on the remaining dough fractions after removing (peeling) the dough from the ATR crystals.

When evaluating the collected data set, a significant effect can be seen as a result of prolonged kneading action (producing sticky dough). As illustrated in Fig. 3D, the amide II band of gluten protein at 1,550  $\text{cm}^{-1}$  increases as an effect of kneading, while the CO/COC stretching band of starch at 1,070  $\text{cm}^{-1}$  mainly shows a decreasing trend (Fig. 3E).

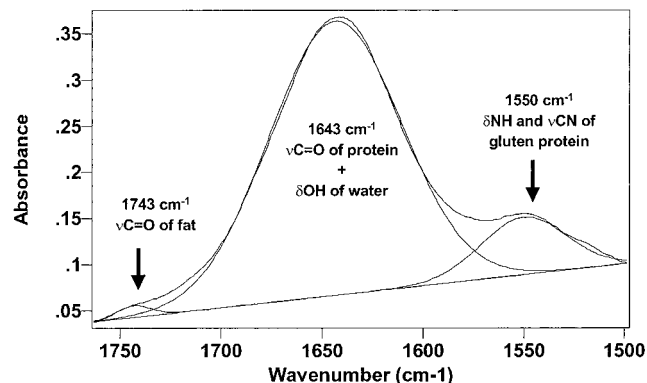


**Fig. 2.** Attenuated total reflectance (ATR) and Fourier transform infrared (FTIR) spectrum (1,800–1,500  $\text{cm}^{-1}$ ) of optimal developed Bacquepi dough (kneaded for 13 min) collected on a ZnSe ATR crystal with a 60° angle of incidence. Curve fitting is applied to resolve infrared bands at 1,745  $\text{cm}^{-1}$  (CO stretch), 1,640  $\text{cm}^{-1}$  (amide I, OH bend), and 1,550  $\text{cm}^{-1}$  (amide II).

Four explanations can be postulated with respect to these observations. 1) Hydration will lead to an increased transition dipole moment of the amide groups, resulting in more intense infrared absorptions. 2) Hydration will lead to a better physical contact between the ZnSe ATR substrate and the (sticky) gluten protein. 3) Hydration will promote the gluten protein to migrate to the upper layers due to an increasing mobility. Consequently, the starch content at the upper layers will decrease, or will be superseded to deeper situated layers. 4) The starch adsorbs water and swells. Therefore this component becomes less concentrated and is therefore less observed. In general, these observations strongly indicate that the hydration of gluten protein plays an important role in the development of a sticky dough.

Another trend was observed when evaluating the sticky and nonsticky dough compositions at three different sampling depths. As shown in Fig. 3A and B, the absorption of fat at  $1,745\text{ cm}^{-1}$  (C=O stretch) and the OH deformation band of water at  $2,150\text{ cm}^{-1}$  show a remarkably opposite surface affinity. The obtained data suggest that fat is preferably located at the outer dough surface, in contrast to water. When peeling the dough from the ATR crystal the opposite effect is observed. As shown in Fig. 3G, the relative amount of fat remaining at the ATR crystal is significantly higher than water (Fig. 3F). Along with surface affinity, this observation provides direct evidence for the relatively weak interaction of fat with the dough. Other than these two major trends, the remaining contour plots in Fig. 3 showed no distinctive relationships. Interpretation of Fig. 3C and H is hampered due to the spectral

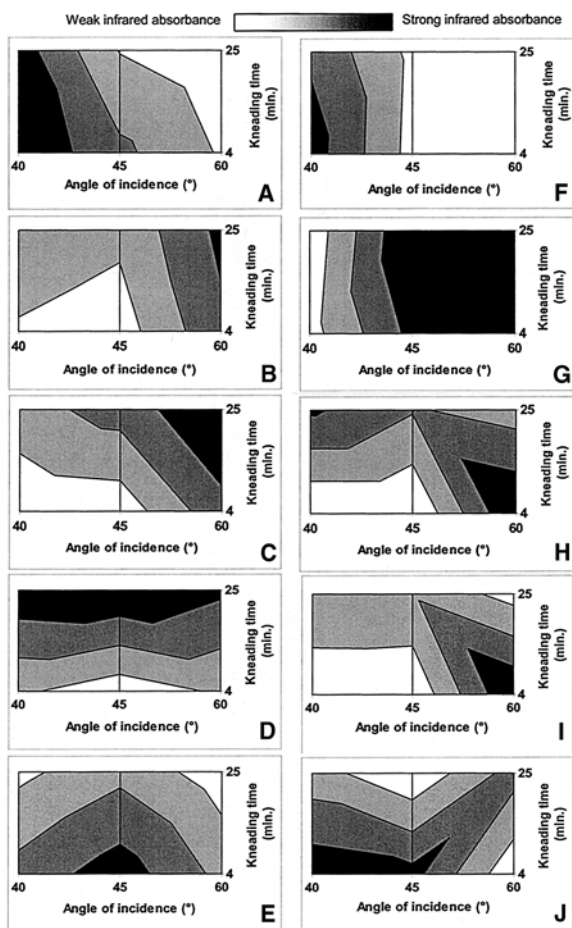


**Fig. 3.** Dough constituent distributions of (A)+(F) water, (B)+(G) fat, (C)+(H) water/gluten protein, (D)+(I) gluten protein, and (E)+(J) starch at dough surfaces depended on sampling depth and kneading time. Measurements were performed (A–E) before and (F–J) after peeling the dough from the ZnSe ATR plates. Approximation of penetration depth at various angles of incidence are given in Table IV.

contribution of gluten protein and water at  $1,640\text{ cm}^{-1}$  (amide I of gluten protein and OH bend of water). Differences in water and protein concentrations, the individual hydration states, and the sensitivity toward infrared radiation makes this combined infrared band rather difficult to interpret.

Furthermore, a different distribution behavior of gluten protein and starch is observed after peeling the sticky and nonsticky dough from the ATR plates. In contrast to the distribution of these constituents in the bulk dough (Fig. 3D and J) distinctive trends are absent. Apparently the relative proportions of gluten protein and starch are severely disrupted as a consequence of manual (irreproducible) peeling. It is expected that the application of a more intelligent peeling approach will lead to more reproducible measurements (Chen and Hoseney 1995; Dobraszcyk 1997; Hoseney and Smewing 1999; Schwazlaff et al 2001).

### Chemical Characterization of Gluten Protein

A series of gluten samples in  $\text{D}_2\text{O}$  were measured on a  $45^\circ$  ZnSe ATR plate to investigate conformational changes in the secondary gluten protein structure as an effect of kneading and stretching. In Fig. 4A, the collected infrared spectra obviously display significant intensity changes in amide I ( $1,640\text{ cm}^{-1}$ ) and amide II ( $1,550\text{ cm}^{-1}$ ) absorptions. Similar to the kneading experiments with dough, these effects can be explained mainly by hydration. Kneading and stretching actions strongly promote protein hydration, which in turn causes 1) an increasing transition dipole moment of the infrared sensitive amide groups; and 2) a better physical contact between the ZnSe ATR substrate and the sticky gluten protein.

To emphasize the spectral features due to conformational changes in the secondary protein structure, curve fitting was applied to resolve four infrared frequencies at  $1,612$ ,  $1,631$ ,  $1,650$ , and  $1,668\text{ cm}^{-1}$  (Fig. 4B). The infrared absorption at  $1,631\text{ cm}^{-1}$  is highly characteristic of amide groups involved in the extended  $\beta$ -sheet structure, while the low-frequency amide I band at  $1,612\text{ cm}^{-1}$  can be associated with the presence of intermolecular  $\beta$ -sheet networks because it occurs readily on aggregate proteins. The prominent band at  $1,650\text{ cm}^{-1}$  is assigned to the  $\alpha$ -helical conformation, although

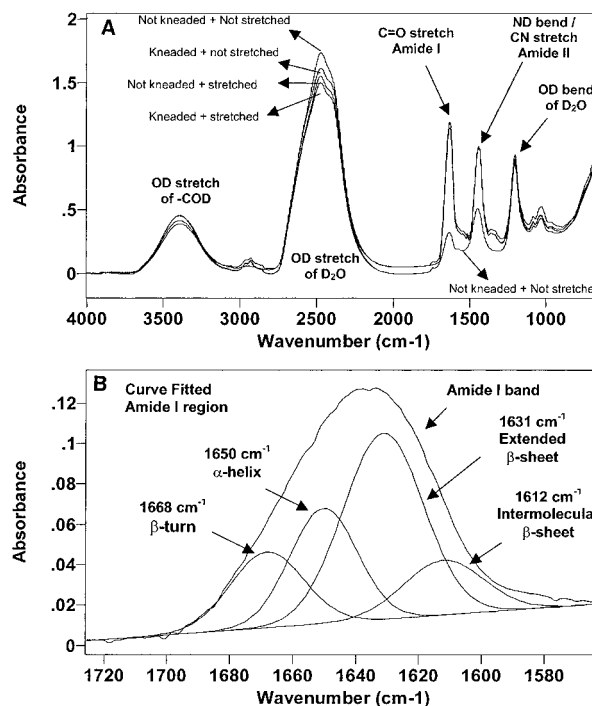


**Fig. 4.** A, Infrared spectra of gluten protein in  $\text{D}_2\text{O}$  as an effect of kneading and stretching, measured at a  $45^\circ$  ZnSe ATR plate. B, Curve-fitted amide I band of gluten protein in  $\text{D}_2\text{O}$  (Pezolet et al 1992).

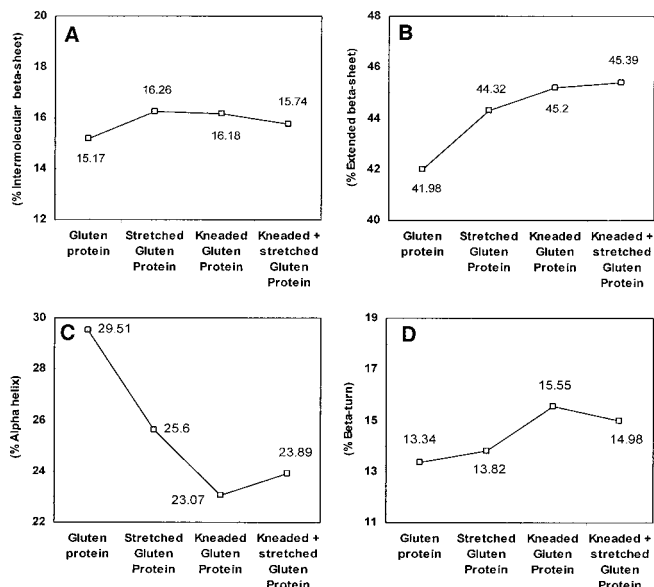


**Fig. 5.** Conformational changes in the secondary protein structure of gluten protein as a result of stretching or kneading. Relative peak areas determined (Pezolet et al 1992) at  $1,612\text{ cm}^{-1}$  of intermolecular  $\beta$ -sheet (A),  $1,631\text{ cm}^{-1}$  of extended  $\beta$ -sheet (B),  $1,650\text{ cm}^{-1}$  of  $\alpha$ -helix (C), and  $1,668\text{ cm}^{-1}$  of  $\beta$ -turn (D). Curve-fitting was applied in the amide I region of infrared spectrum to resolve overlapping structure elements.

the spectral contribution from the unordered conformation cannot be completely ruled out at this frequency. Finally, the  $1,668\text{ cm}^{-1}$  band is assigned to the  $\beta$ -turn conformation (Pezolet et al 1992; Popineau et al 1994; Belton 1999). The method of Pezolet et al (1992) has been used to quantify the secondary structure elements in the gluten protein. The results obtained with this method (Fig. 5) show that gluten protein contains mainly relatively high fractions of  $\beta$ -sheets. Reasonable differences were observed when the gluten proteins were kneaded and stretched before infrared analysis in comparison with freshly prepared (moistened) gluten. It appears that kneading and stretching mainly result in a decreasing amount of  $\alpha$ -helices (Fig. 5C) accompanied by increased content of the extended  $\beta$ -sheet conformations (Fig. 5B).

## DISCUSSION AND CONCLUSIONS

The important role of gluten proteins with respect to dough stickiness was established by ATR FTIR spectroscopy. Using ATR FTIR, spectral information was obtained from the outer dough surface ( $0.5\text{--}4\text{ }\mu\text{m}$ ). Depending on the hydration state of the gluten protein, relatively higher amide intensities were measured at dough surfaces compared with starch and water. It was established experimentally that changes in relative amide band intensities can be explained by changes in the transition dipole moment. Based on these observations, hydrated gluten might be one of the major contributors to dough stickiness.

Along with gluten protein, fat also shows a relatively strong surface affinity. However, when applying a peeling test at an ATR plate, fat shows a relatively weak affinity with dough. This might indicate that fat is probably not the dominating factor in dough stickiness.

When analyzing gluten protein in  $\text{D}_2\text{O}$  instead of a dough matrix, more or less similar results were obtained. Significant differences in the amide intensities were measured for kneaded or stretched protein gluten in comparison with the wet, untreated gluten. In addition to changes in band intensities, conformational changes were also quantified. It appears that kneading and stretching results in a decrease of the amount of  $\alpha$ -helices accompanied by an increase of the content of the extended  $\beta$ -sheet conformations.

## ACKNOWLEDGMENTS

We thank R. de Man and K. van der Linden for preparing the dough samples and Y. Nicolas for assistance with the infrared measurements and the stimulating discussions.

## LITERATURE CITED

- Belton, P. S. 1999. On the elasticity of wheat gluten. *J. Cereal Sci.* 29:103-107.
- Byler, D. M., Bouillette, J. N., and Susi, H. 1986. Quantitative studies of protein structure by FTIR spectral deconvolution and curve fitting. *Spectroscopy* 3:29-32.
- Chen, W. Z., and Hosoney, R. C. 1995. Development of an objective method for dough stickiness. *Lebensm. Wiss. Technol.* 28:467-473.
- Dobraszczyk, B. L. 1997. The rheological basis of dough stickiness. *J. Texture Stud.* 28:139-162.
- Dupuy, N., Duponchel, L., Amram, B., Huvenne, J. P., and Legrand, P. 1994. Quantitative analysis of latex in paper coatings by ATR-FTIR spectroscopy. *J. Chemometrics* 8:333-347.
- Harrick, N. 1979. *Internal Reflection Spectroscopy*. Harrick Scientific Corp.: Ossining, NY.
- Hosoney, H. C., and Smewing, J. 1999. Instrumental measurement of stickiness of doughs and other foods. *J. Texture Stud.* 30:123-136.
- Mangavel, C., Carre, P., Sanchez, A. C., Barbot, J., Popineau, Y., and Gueguen, J. 1998. Film formation from wheat gluten proteins: A Fourier transform infrared spectroscopic study. *Biopolym. Sci. Food Non Food Appl.* 1:257-261.
- Mantsch, H. H., and Casal, H. L. 1986. Biological applications of infrared spectrometry. *Fresenius Z. Anal. Chem.* 324:655-661.
- Martin, K. 1999. Infrared and Raman studies of skin and hair: A review of cosmetic spectroscopy. *Int. J. Vib. Spectrosc.* 3:1-21.
- Pezolet, M., Bonenfant, S., Dousseau, F., and Popineau, Y. 1992. Conformation of wheat gluten proteins—Comparison between functional and solution states as determined by infrared spectroscopy. *FEBS Lett.* 3:247-250.
- Popineau, Y., Bonenfant, S., Cornec, M., and Pezolet, M. 1994. A study by infrared spectroscopy of the conformations of gluten proteins differing in their gliadin and glutenin compositions. *J. Cereal Sci.* 20:15-22.
- Schwazlaff, S. S., Uriyo, M. G., Johnson, J. M., Barbeau, W. E., and Griffey, C. A. 2001. Apparent dough stickiness of selected 1BL/1RS translocated soft wheat flours. *Cereal Chem.* 78:93-96.
- Tatham, S. A., Drake, A. F., and Shewry, P. R. 1990. Conformational studies of synthetic peptides corresponding to the repetitive regions of the high molecular weight (HMW) glutenin subunits of wheat. *J. Cereal Sci.* 11:189-200.
- van de Voort, F. R., and Ismail, A. A. 1991. Proximate analysis of foods by mid-FTIR spectroscopy. *Trends Food Sci. Technol.* 13-17.
- Wharton, C. W. 1986. Infra-red and Raman spectroscopic studies of enzyme structure and function. *J. Biochem.* 233:25-36.
- Wilson, R. H. 1990. Fourier transform mid-infrared spectroscopy for food analysis. *Trends Anal. Chem.* 9:127-131.
- Workman, J. 2001. Methods and interpretations. Pages 209-242 in: *Handbook of Organic Compounds*. Academic Press: London.

[Received January 11, 2002. Accepted November 19, 2002.]